Letter

# Skyrmion lattice annihilation by point defects in the multiferroic $Cu_2OSeO_3$

Houssam Sabri* and Igor Kornev
*Laboratoire SPMS UMR 8580, Université Paris-Saclay, CentraleSupélec, CNRS, 91190 Gif-sur-Yvette, France*

(Received 20 June 2023; accepted 18 September 2023; published 2 October 2023)

First-principles-based effective Hamiltonian simulations are used to reveal the hidden connection between various topological defects, namely point defects and skyrmions, in copper oxide selenite ($Cu_2OSeO_3$). Using this approach, we show that (i) $Cu_2OSeO_3$ hosts different topological defects with a nonzero local topological charge in various regions of the magnetic-field–temperature phase diagram $(H, T)$, (ii) point defects exert external pressure on skyrmions leading to their gradual annihilation as temperature increases, and (iii) this annihilation of skyrmions is a result of the melting of the lattice into a glassylike state of spins that connects with the paramagnetic phase.

DOI: 10.1103/PhysRevB.108.L140401

*Introduction*. Topological defects arise in a wide variety of condensed matter systems, and due to their nature related to the topological properties, interest in the field of spintronics has surged. The potential of devices based on topological defects, especially skyrmions, has gained the attention of the condensed matter community in the last decade. A direct result of topological defects' topological stability is their robustness in the presence of continuous mechanical deformations and defects, leading to extensive studies of the topological solitons in magnetic materials, including vortices, hedgehogs, and skyrmions. Skyrmions were first proposed by Skyrme in 1962 in the field of particle physics to describe a solution of the nonlinear field in dense nuclear matter [1]. After that, the concept of skyrmions has been found in various condensed matter systems, such as liquid crystals [2], quantum Hall systems [3], and magnetic materials. Magnetic skyrmions are the primary example of topological spin textures. They are characterized by a topological invariant called the skyrmion number $\mathcal{Q}_{sk}$, which describes the local configuration of how the vector field of magnetic dipoles whirls in the plane. The magnetic skyrmions were expected to exist within magnetic materials with strong Dzyaloshinskii-Moriya interaction (DMI) [4,5]. They were first discovered in the metallic noncentrosymmetric chiral cubic MnSi [6]. This started the hunt for skyrmions in other B20 crystals such as FeGe [7] and $Fe_{1-x}Co_xSi$ [8], and they were found in both bulk material and thin films [9]. These spin textures, called skyrmions, are nontrivial topological configurations that can be described as circular spin textures with an up spin on the edge of the circle and a down spin in the center. In between, there is a smooth transition with topological features. Furthermore, magnetic skyrmions were found in multiferroic copper oxide selenite ($Cu_2OSeO_3$) with the cubic space group $P2_13$ as for B20 magnets [10]. Skyrmions in bulk $Cu_2OSeO_3$ and bulk B20 magnets exist in a narrow pocket of the magnetic-field–temperature phase diagram; however, isolated skyrmions are hard to stabilize, and thus in $Cu_2OSeO_3$ the magnetic skyrmions are arranged in a hexagonal two-dimensional (2D) lattice called the skyrmion lattice (SkL) phase.

There are several methods to characterize topological defects; in the case of 2D solitons such as vortices and skyrmions, the skyrmion number is defined as [11]

$$\mathcal{Q}_{sk} = \frac{1}{4\pi}\int_{\mathbb{R}^2} \mathbf{m}\cdot\left(\frac{\partial \mathbf{m}}{\partial x}\times\frac{\partial \mathbf{m}}{\partial y}\right)dxdy, \quad \mathbf{m} = \frac{\mathbf{M}}{|\mathbf{M}|}, \tag{1}$$

where $\mathbf{m}$ is the normalized local magnetization.

This Research Letter aims to quantify the topological properties of different solitons in $Cu_2OSeO_3$ from first principles. We define the different significant topological quantities and calculate the charge of every soliton on the phase diagram of $Cu_2OSeO_3$ (skyrmion lattice phase, vortex lattice, and helical state). We also seek to isolate topological entities such as hedgehogs and antihedgehogs (point defect in three dimensions) and study their interaction with skyrmions. We numerically access the temperature evolution of the density $n_\pm$ of topological point defects (sum of the density of hedgehogs and antihedgehogs) and the spin configurations at different temperatures and magnetic fields.

*Methods*. We use first-principles density functional theory (DFT) calculations with the Vienna *ab initio* simulation package (VASP) [12] to parametrize our effective Hamiltonian model. The pseudopotentials adopt the projector augmented-wave method, with the generalized gradient approximation [13] used as the exchange-correlation functional, and the $U$ correction was added for the copper ions to account for the strong correlation properties of $3d$ electrons [14,15]. Monte Carlo simulations were performed to study the behavior at finite temperatures, which relies on the Metropolis algorithm [16,17] inside an $84\times84\times84$ cubic supercell with periodic boundary conditions and contains $\sim10^7$ spins. We used $5\times10^5$ sweeps to equilibrate the system and then $5\times10^5$ sweeps to get the various statistical averages. The calculations begin at a high temperature from a random

*houssam.sabri@centralesupelec.fr

 

configuration, and the temperature is then decreased in small steps to get well-converged results. We note that the effective Hamiltonian employed to simulate the properties of $Cu_2OSeO_3$ [18] yields the same characteristic phase diagram reported in previous experimental studies [10,19]. The energy of the magnetic effective Hamiltonian is written as

$$E_{\text{total}}(\{\mathbf{S}\}) = \sum_{i<j}\left[J_w^{\text{FM}}\mathbf{S}_i\cdot\mathbf{S}_j + J_s^{\text{AFM}}\mathbf{S}_i\cdot\mathbf{S}_j + J_s^{\text{FM}}\mathbf{S}_i\cdot\mathbf{S}_j + J_w^{\text{AFM}}\mathbf{S}_i\cdot\mathbf{S}_j + J_O^{\text{AFM}}\mathbf{S}_i\cdot\mathbf{S}_j\right] + \sum_{i<j}\left[\mathbf{D}_w^{\text{FM}}\cdot\mathbf{S}_i\times\mathbf{S}_j + \mathbf{D}_s^{\text{AFM}}\cdot\mathbf{S}_i\times\mathbf{S}_j + \mathbf{D}_s^{\text{FM}}\cdot\mathbf{S}_i\times\mathbf{S}_j + \mathbf{D}_w^{\text{AFM}}\cdot\mathbf{S}_i\times\mathbf{S}_j + \mathbf{D}_O^{\text{AFM}}\cdot\mathbf{S}_i\times\mathbf{S}_j\right] + \sum_i g_S\frac{\mu_B}{\hbar}\mathbf{S}_i\cdot\mathbf{B}_{\text{ext}}, \tag{2}$$

where $J_s$ ($J_w$) are the different ferromagnetic and antiferromagnetic strong (weak) Heisenberg interactions in our system, with $\mathbf{D}$ being the equivalent Dzyaloshinskii-Moriya interaction (DMI) vector, and $J_O$ is the only superexchange interaction (long-range coupling mediated by the bridging oxo ligand) with its corresponding DMI vector $\mathbf{D}_O$. The values of the different interactions are the same as in our previous study [18].

*Topological quantities*. Following the approach by Berg and Lüscher [20] (see also Ref. [21]), we define the skyrmion number in the case of lattice systems. For a plane of four spins, the topological charge is given by the sum over the ensemble of oriented triangles $\Delta_{ijk}$. We calculate first the local charge $q_\Delta$ of the triangle $\Delta_{ijk}$ with respect to the chosen orientation. The skyrmion number can be extracted from the local charge by summing on the whole space (in the case of 2D solitons as skyrmions and vortices, we sum over the 2D surface), and the lattice-based formula for the skyrmion number is (see Supplemental Material [22] for details)

$$\mathcal{Q}_{sk} = \frac{1}{4\pi}\sum_{\Delta=\langle ijk\rangle} q_\Delta. \tag{3}$$

In order to quantify 3D point defects (hedgehogs and antihedgehogs) with charge $\mathcal{Q}_\pm$, we use the procedure of Motrunich and Vishwanath [23]. The hedgehog (antihedgehog) topological charge $\mathcal{Q}_+$ ($\mathcal{Q}_-$) enclosed by the unit cube containing six squares can be written as follows:

$$\mathcal{Q}_\pm = \frac{1}{2\pi}\sum_{\square=1}^{6}\mathsf{F}_\square, \tag{4}$$

where $\mathsf{F}_\square$ is the flux of a cube face. This charge is guaranteed to be an integer from the definition and ensures that the net topological charge (the supercell sum of topological charges associated with unit cells) always equals zero in the considered system with periodic boundary conditions (details of the derivation of the charge can be found in the Supplemental Material [22]).

*Results*. We first analyze the topological skyrmion number for the zero-field case, where we have a helical state at lower temperatures and then a transition to the fluctuation-disordered (FD) phase that exists in the temperature range 37.5–42.25 K [18]. We find, as shown in Fig. 1(a), that the helical state is, as expected, topologically trivial and is characterized with $\mathcal{Q}_{sk} = 0$. This, in particular, means that the DMI itself does not create the net topological charge, and it needs the magnetic field to break the symmetry in agreement with the work of Hou *et al.* [24]. However, as we enter the FD region of temperatures, the strong spin fluctuations make the skyrmion number fluctuate around the trivial state.

We analyze the skyrmion number for (111) planes in an applied magnetic field $\mathbf{B}_{\text{ext}} = 40$ mT along the (111) direction. We find that the skyrmion number stays zero for lower temperatures where the trivial conical phase is stable. It

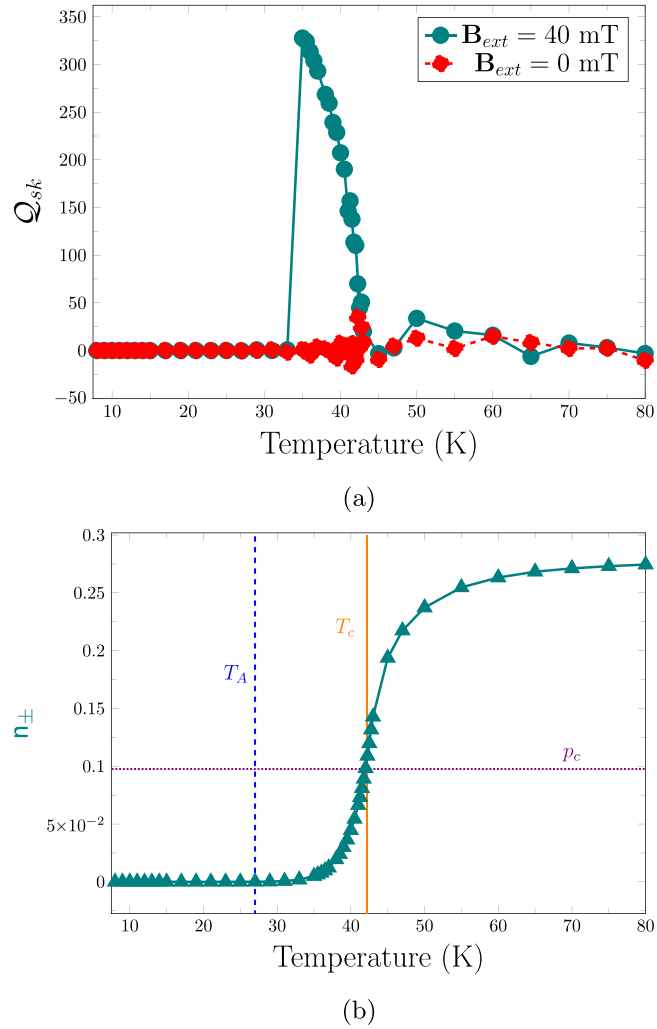


FIG. 1. (a) Dashed line, skyrmion number $\mathcal{Q}_{sk}$ along the conical-SkL-FD-paramagnetic transition; solid line, skyrmion number $\mathcal{Q}_{sk}$ along the helical-FD-paramagnetic transition. (b) Density of the cells with point defects $\mathsf{n}_\pm$ as a function of temperature, where $p_c$ is the percolation threshold of a Rubik's cube environment and $T_A$ is the point defects' activation temperature.

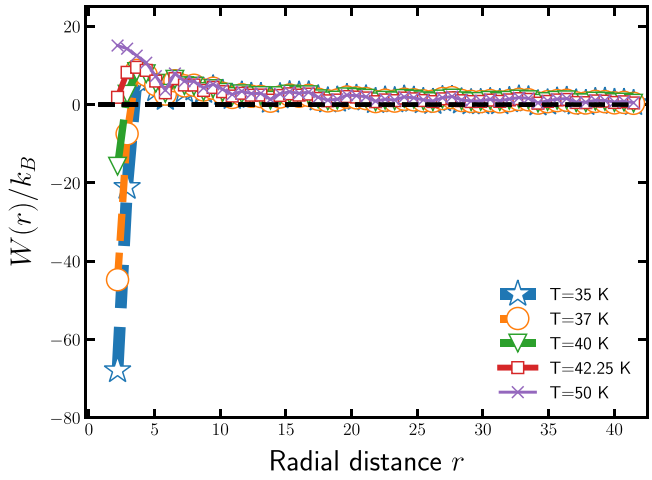


FIG. 2. The pairwise potential between point defects $W(r)$ for various temperatures ($T_c = 42.25$ K), where we observe the changing nature from an attractive potential for $T < T_c$ to a repulsive potential for $T \geqslant T_c$.

increases steeply to the maximum as we enter the skyrmion lattice phase and then decreases smoothly with a slower rate and small fluctuations due to the FD regime [19]. In the paramagnetic phase ($T > T_c = 42.25$ K), we have fluctuation of the skyrmion number around the value of zero; such behavior was previously found in ultrathin films of Pd/Fe/Ir(111) [25]. Let us now define the density $\mathsf{n}_\pm$ of topological defects as the ratio of cells containing hedgehogs or antihedgehogs to the supercell volume $L^3$ with $L = 84$. Figure 1(b) shows the thermal evolution of the density of hedgehog-antihedgehog pairs. The density $\mathsf{n}_\pm$ is found to decrease smoothly with decreasing temperature until an activation temperature $T_A$ where the density is precisely zero. It is striking to realize that the critical temperature $T_c$ is the inflection temperature of the hedgehogs' density, which also coincides with the site-percolation threshold of a Rubik's cube neighborhood $p_c$. The site-percolation threshold $p_c$ is that of a regular lattice with a neighborhood extending to the third-nearest neighbors (Rubik's-cube-like) $p_c = 0.0976$ [26]. This threshold can be seen as the critical probability above which we have the appearance of a single cluster of topological defects spanning over the whole supercell ("infinite cluster"). This behavior of point defects was previously found in relaxor ferroelectric $Pb(Sc_{0.5}Nb_{0.5})O_3$ (PSN) and $Ba(Zr_{0.5}Ti_{0.5})O_3$ (BZT) systems [27] and in Heisenberg ferromagnets [28,29]. The nonvanishing value of the point defects' density under $T_c$ indicates the coexistence of hedgehog-antihedgehog pairs alongside the skyrmion lattice phase in the case of an applied 40 mT magnetic field. This means that if the density of hedgehog-antihedgehog pairs $\mathsf{n}_\pm > p_c$, the appearance of a long-range spin configuration is hindered by the infinite cluster of topological point defects.

We compute the radial distribution function $g(r)$, used to extract the mean-force potential between defects $W(r) = -k_B T \ln(g(r))$ as well as using the $K$-means clustering method to explore the evolution of point defect clusters. Figure 2 shows the evolution of the mean-force potential between defects $W(r)$ as a function of temperature. We observe that

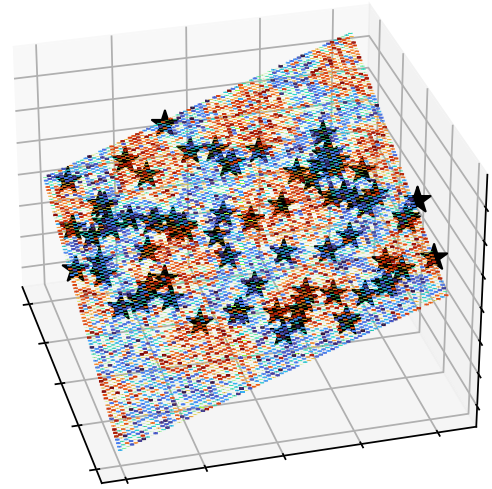

(a)

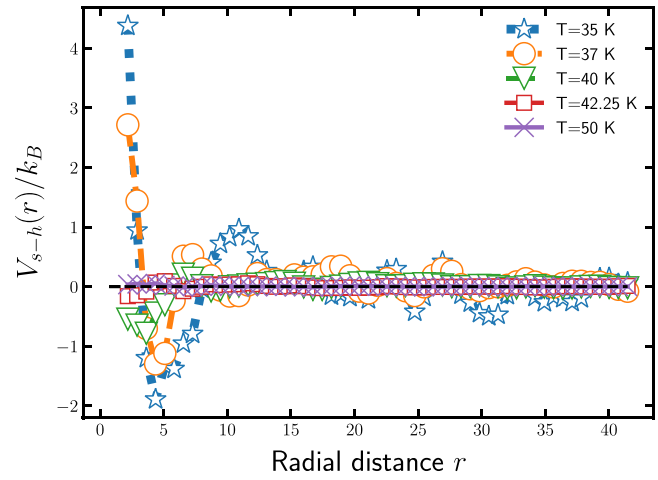


(b)

FIG. 3. (a) Point defects' (black stars) distribution in a (111) plane in the presence of the skyrmion lattice phase ($\mathbf{B}_{\text{ext}} = 40$ mT and $T = 37$ K) where point defects are clustered in the space between skyrmions (in red). (b) The interaction potential between skyrmions and point defects $V_{s\text{-}h}(r)$ for various temperatures ($T_c = 42.25$ K) as calculated from the radial distribution function, where $V_{s\text{-}h}(r)$ has a glassylike behavior until $V_{s\text{-}h}(r) = 0$ for $T \geqslant T_c$ due the total vanishing of skyrmions.

point defects repel each other for high temperatures and cannot easily be close to each other lest they overlap the nearest hedgehogs. As the temperature decreases below $T_c$, the pairwise potential $W(r)$ becomes slightly attractive, and clusters begin to form. The radial distribution function obtained at these temperatures significantly differs from that obtained at $T \geqslant 50$ K, implying that the point defects' behavior (as individual particles) is also very different. At this density of point defects, the depletion forces can be described by the Asakura and Oosawa model [30,31], which predicts a monotonically attractive potential. In this temperature range, point defects are in the subpercolation regime, where $\mathsf{n}_\pm < p_c$ and point defects form separated structured clusters as depicted

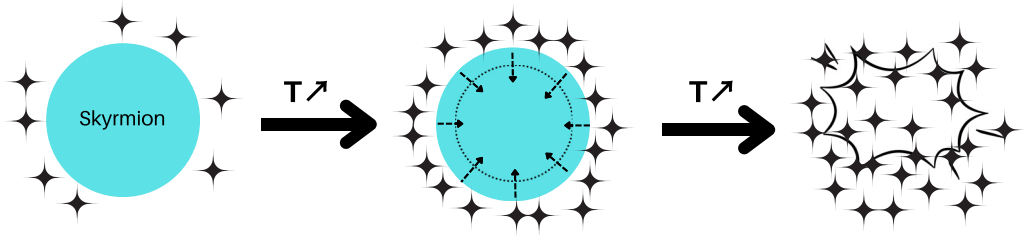


FIG. 4. Schematic representation of the process of skyrmion annihilation by the point defects (black stars) showing the gradual destruction of the skyrmion as a result of the increasing applied pressure of hedgehog-antihedgehog pairs, which is due to the increasing density of point defects in the space between skyrmions as temperatures increase, leading to total destruction of the skyrmion phase as we enter the paramagnetic phase.

in Fig. 3(a). In other words, point defects become trapped in a cage formed by their neighbors, similar to a glassy state of particles. The pairwise potential becomes even more attractive as we reduce temperatures and get closer to the activation temperature $T_A$.

Interestingly, since the total topological charge is constrained to be zero in systems with periodic boundary conditions, the decrease of $\mathsf{n}_\pm$ upon cooling can only happen by annihilation among defects of opposite topological charge, i.e., between hedgehogs with charge $\mathcal{Q}_+$ and antihedgehogs with charge $\mathcal{Q}_-$. For the dependence of $\mathsf{n}_\pm$ on temperature in Fig. 1(b), we find that for $T > T_A$, the density can be very well approximated by

$$\mathsf{n}_\pm = \mathsf{n}_\pm^0 + (\mathsf{n}_\pm^\infty - \mathsf{n}_\pm^0)\exp\left(-\frac{A}{T-T_A}\right). \tag{5}$$

This leads to the Vogel-Fulcher-Tammann-law-like equation for relaxation time $\tau$ associated with the annihilation process between hedgehogs and antihedgehogs, $\tau \sim \tau_0 \exp(\frac{A}{T-T_A})$ [32], which is the same equation used to model viscosity near the glass transition as in the glassy state behavior evoked in the previous paragraph.

An important question about the role of topological defects is whether the observed proliferation of point defects, as $T$ increases, is accompanied by an unbinding of defect pairs. For that, we calculated the number of total bonds as a function of temperature and the number of bonds at the minimal distance as a function of temperature. It is thus essential to develop criteria by which a given system is in a bound or unbound hedgehog state. The ratio of the bonds at the minimum distance to the total bonds will give an idea about the binding-unbinding mechanism of hedgehog-antihedgehog pairs occurring in $Cu_2OSeO_3$. In our case, we observe a decreasing ratio with increasing temperatures, which means that the pairs tend to unbind, rendering the gas of defects into a plasmalike state of hedgehogs and antihedgehogs. This unbinding mechanism is also shown in Fig. 2 by the pairwise potential $W(r)$ changing in nature from attractive to repulsive as we pass from $T < T_c$ to $T > T_c$. Although the nature of the total pairwise potential stays the same in the absence (at 0 mT) and in the presence (at 40 mT) of the skyrmion lattice phase, being attractive in $T < T_c$ and repulsive in $T > T_c$, the existence of the skyrmions adds an additional component to the pairwise potential, which can be interpreted as the interaction potential between skyrmions and point defects $V_{s\text{-}h}(r)$. This potential can be extracted by comparing the pairwise potential of point defects in the presence and absence of skyrmions.

$$V_{s\text{-}h}(r) = W(r)_{\mathbf{B}_{\rm ext}=40\,\rm mT} - W(r)_{\mathbf{B}_{\rm ext}=0\,\rm mT}. \tag{6}$$

Figure 3(b) shows the evolution of the interaction potential between skyrmions and point defects (hedgehogs and antihedgehogs) and exhibits the behavior of the periodic structure (solidlike) melting into a liquidlike potential as the temperature increases, until we have no interaction above $T_c$ due to total annihilation of skyrmions. To understand the effect of point defect clusters on the skyrmion lattice, we analyzed how the point defects are scattered on the (111) plane in the presence of skyrmions. As seen previously, in a magnetic field of 40 mT applied along the (111) direction, a skyrmion lattice phase emerges near $T_c$. In the presence of skyrmions, the point defects are arranged in clusters in the space between skyrmions, which can be related to $V_{s\text{-}h}$ being attractive in these distances (between skyrmions) as shown in Fig. 3(a), leading to applied pressure by point defects on skyrmions. As the temperature increases, the point defects' density grows. The point defects exert increasing pressure as the temperature rises, leading to annihilation of the skyrmion lattice phase. This process of skyrmion annihilation by the point defects is schematically depicted in Fig. 4. We observe that the applied pressure gradually reduces the total skyrmion charge until the complete annihilation of the skyrmion lattice phase. The potential $V_{s\text{-}h}$ in Fig. 3(b) shows the behavior of a gradual melting of the skyrmion lattice phase as a result of the pressure of point defects; hence there is a gradual decrease in the skyrmion number $\mathcal{Q}_{sk}$ as temperatures increase toward $T_c$ as previously seen in Fig. 1(a). The impact of point defects on the annihilation of skyrmions during the helical-to-skyrmion-lattice or conical-to-skyrmion-lattice transition was previously seen in a study by Birch *et al.* [33], where they demonstrated that Bloch points, a specific type of three-dimensional point defect, facilitated the creation and annihilation of skyrmions under a magnetic field in $(Cu_{1-x}Zn_x)_2OSeO_3$.

In contrast, our study investigates the role of point defects in eliminating the skyrmion lattice phase as the temperature rises and $Cu_2OSeO_3$ transitions to the paramagnetic phase. In essence, our findings reveal the influence of the proliferation of three-dimensional point defects on the annihilation of ordered phases, particularly the melting and annihilation of the skyrmion lattice phase as a result of the pressure applied by point defects.

*Acknowledgments.* The authors are grateful for support provided by NVIDIA via an NVIDIA GPU Grant. This work was performed using high-performance computing resources from the "Mésocentre" computing center of CentraleSupélec and École Normale Supérieure Paris-Saclay supported by CNRS and Région Île-de-France [34]. This project has received funding from the European Union's Horizon 2020 research and innovation program under Grant Agreement No. 964931 (TSAR).

[1] T. Skyrme, A unified field theory of mesons and baryons, Nucl. Phys. **31**, 556 (1962).
[2] A. Bogdanov, U. Rößler, and A. Shestakov, Skyrmions in nematic liquid crystals, Phys. Rev. E **67**, 016602 (2003).
[3] L. Brey, H. Fertig, R. Côté, and A. MacDonald, Skyrme Crystal in a Two-Dimensional Electron Gas, Phys. Rev. Lett. **75**, 2562 (1995).
[4] I. Dzyaloshinsky, A thermodynamic theory of "weak" ferromagnetism of antiferromagnetics, J. Phys. Chem. Solids **4**, 241 (1958).
[5] T. Moriya, Anisotropic superexchange interaction and weak ferromagnetism, Phys. Rev. **120**, 91 (1960).
[6] S. Mühlbauer, B. Binz, F. Jonietz, C. Pfleiderer, A. Rosch, A. Neubauer, R. Georgii, and P. Böni, Skyrmion lattice in a chiral magnet, Science **323**, 915 (2009).
[7] X. Yu, N. Kanazawa, Y. Onose, K. Kimoto, W. Zhang, S. Ishiwata, Y. Matsui, and Y. Tokura, Near room-temperature formation of a skyrmion crystal in thin-films of the helimagnet FeGe, Nat. Mater. **10**, 106 (2011).
[8] W. Münzer, A. Neubauer, T. Adams, S. Mühlbauer, C. Franz, F. Jonietz, R. Georgii, P. Böni, B. Pedersen, M. Schmidt, A. Rosch, and C. Pfleiderer, Skyrmion lattice in the doped semiconductor $Fe_{1-x}Co_xSi$, Phys. Rev. B **81**, 041203(R) (2010).
[9] X. Yu, Y. Onose, N. Kanazawa, J. Park, J. Han, Y. Matsui, N. Nagaosa, and Y. Tokura, Real-space observation of a two-dimensional skyrmion crystal, Nature (London) **465**, 901 (2010).
[10] S. Seki, X. Yu, S. Ishiwata, and Y. Tokura, Observation of skyrmions in a multiferroic material, Science **336**, 198 (2012).
[11] S. Heinze, K. Bergmann, M. Menzel, J. Brede, A. Kubetzka, R. Wiesendanger, G. Bihlmayer, and S. Blügel, Spontaneous atomic-scale magnetic skyrmion lattice in two dimensions, Nat. Phys. **7**, 713 (2011).
[12] G. Kresse and J. Furthmüller, Efficient iterative schemes for *ab initio* total-energy calculations using a plane-wave basis set, Phys. Rev. B **54**, 11169 (1996).
[13] J. Perdew, K. Burke, and M. Ernzerhof, Generalized Gradient Approximation made Simple, Phys. Rev. Lett. **77**, 3865 (1996).
[14] V. Anisimov, J. Zaanen, and O. Andersen, Band theory and Mott insulators: Hubbard $U$ instead of Stoner $I$, Phys. Rev. B **44**, 943 (1991).
[15] S. Dudarev, G. Botton, S. Savrasov, C. Humphreys, and A. Sutton, Electron-energy-loss spectra and the structural stability of nickel oxide: An LSDA+U study, Phys. Rev. B **57**, 1505 (1998).
[16] N. Metropolis and S. Ulam, The Monte Carlo method, J. Am. Stat. Assoc. **44**, 335 (1949).
[17] W. Hastings, Monte Carlo sampling methods using Markov chains and their applications, Biometrika **57**, 97 (1970).
[18] H. Sabri and I. Kornev, Monte Carlo studies of noncollinear magnetic phases in multiferroic $Cu_2OSeO_3$, Phys. Rev. B **107**, 024417 (2023).
[19] H. Chauhan, B. Kumar, J. Tiwari, and S. Ghosh, Multiple phases with a tricritical point and a Lifshitz point in the skyrmion host $Cu_2OSeO_3$, Phys. Rev. B **100**, 165143 (2019).
[20] B. Berg and M. Lüscher, Definition and statistical distributions of a topological number in the lattice O(3) $\sigma$-model, Nucl. Phys. B **190**, 412 (1981).
[21] J. Kim and J. Mulkers, On quantifying the topological charge in micromagnetics using a lattice-based approach, IOP SciNotes **1**, 025211 (2020).
[22] See Supplemental Material at http://link.aps.org/supplemental/10.1103/PhysRevB.108.L140401 for mathematical details of the topological quantities.
[23] O. Motrunich and A. Vishwanath, Emergent photons and transitions in the O(3) sigma model with hedgehog suppression, Phys. Rev. B **70**, 075104 (2004).
[24] W. T. Hou, J.-X. Yu, M. Daly, and J. Zang, Thermally driven topology in chiral magnets, Phys. Rev. B **96**, 140403(R) (2017).
[25] M. Böttcher, S. Heinze, S. Egorov, J. Sinova, and B. Dupé, $B$–$T$ phase diagram of Pd/Fe/Ir(111) computed with parallel tempering Monte Carlo, New J. Phys. **20**, 103014 (2018).
[26] Ł. Kurzawski and K. Malarz, Simple cubic random-site percolation thresholds for complex neighbourhoods, Rep. Math. Phys. **70**, 163 (2012).
[27] Y. Nahas, S. Prokhorenko, I. Kornev, and L. Bellaiche, Topological Point Defects in Relaxor Ferroelectrics, Phys. Rev. Lett. **116**, 127601 (2016).
[28] S. Ostlund, Interactions between topological point singularities, Phys. Rev. B **24**, 485 (1981).
[29] M. Lau and C. Dasgupta, Numerical investigation of the role of topological defects in the three-dimensional Heisenberg transition, Phys. Rev. B **39**, 7212 (1989).
[30] S. Asakura and F. Oosawa, On interaction between two bodies immersed in a solution of macromolecules, J. Chem. Phys. **22**, 1255 (1954).
[31] C. Bechinger, D. Rudhardt, P. Leiderer, R. Roth, and S. Dietrich, Understanding Depletion Forces Beyond Entropy, Phys. Rev. Lett. **83**, 3960 (1999).
[32] L. Garca-Coln, L. Castillo, and P. Goldstein, Theoretical basis for the Vogel-Fulcher-Tammann equation, Phys. Rev. B **40**, 7040 (1989).
[33] M. Birch, D. Cortés-Ortuño, N. Khanh, S. Seki, A. Štefančič, G. Balakrishnan, Y. Tokura, and P. Hatton, Topological defect-mediated skyrmion annihilation in three dimensions, Commun. Phys. **4**, 175 (2021).
[34] http://mesocentre.centralesupelec.fr/.